ChemPubSoc Europe

DOI: 10.1002/chem.201602981

CHEMISTRY A European Journal Full Paper

Fluorescent Amyloid Probe

Benzothiazole-Based Neutral Ratiometric Fluorescence Sensor for Amyloid Fibrils

Aruna K. Mora,[a] Sushant Murudkar,[a] A. Alamelu,[a, c] Prabhat K. Singh,[a] Subrata Chattopadhyay,[b] and Sukhendu Nath*[a]

Abstract: Early detection of amyloid fibrils is very important for the timely diagnosis of several neurological diseases. Thioflavin-T (ThT) is a gold standard fluorescent probe for amyloid fibrils and has been used for the last few decades. However, due to its positive charge, ThT is incapable of crossing the blood–brain barrier and cannot be used for in vivo imaging of fibrils. In the present work, we synthesized a neutral ThT derivative, 2-[2′-Me,4′-(dimethylamino)phenyl]benzothiazole (2Me-DABT), which showed a strong affinity towards the amyloid fibrils. On association with the amyloid fibrils, 2Me-DABT not only showed a large increase in its emission intensity, but also, unlike ThT, a large blueshift in its emission spectrum was observed. Thus, unlike ThT, 2Me-DABT is a potential candidate for the ratiometric sensor of the amyloid fibrils. Detailed photophysical properties of 2Me-DABT in amyloid fibrils and different solvent media were studied to understand its sensory activity. Fluorescence resonance energy transfer (FRET) studies suggested that the sites of localization for ThT and 2Me-DABT in amyloid fibrils are not same and their average distance of separation in amyloid fibrils was determined. The experimental data was nicely supported by molecular docking studies, which confirmed the binding of 2Me-DABT in the inner core of the amyloid fibrils.

Introduction

Amyloidosis, a pathological condition, arises from the deposition of protein agglomerates on organs and tissues in the human body, and is responsible for several diseases, like, Parkinson's disease, Alzheimer's disease, Huntington's disease, type II diabetes, etc.[1–3] Such protein agglomerates, generally known as amyloid fibrils, are insoluble in water and remarkably resistant towards proteolysis.[4,5] Early detection of amyloidosis and knowledge of its progress is very important to prevent formation of amyloid fibrils in the human body and to develop suitable therapeutics.

Since its discovery by Rudolph Virchow in the year of 1854,[6] several biochemical and biophysical techniques have been used extensively to study amyloid fibrils. Further, light scattering,[7] X-ray scattering,[8] FTIR,[9] and AFM,[10] etc. have been used to compliment the biophysical and biochemical results. However, all such studies were limited to the in vitro and ex vivo experiments. Several imaging techniques, like, magnetic resonance imaging (MRI),[11,12] positron emission tomography (PET),[13,14] and single-photon emission computed tomography (SPECT)[15,16] have been used to study amyloid fibrils deep inside the tissue. Indeed, the first human clinical trial to study amyloidosis was performed by a PET technique using a ^{18}F-labeled radiotracer.[13] However, the use of these techniques is limited by several factors, such as expensive instruments, the radiotracer's short lifetime, complicated data analysis, and, most importantly, exposure to radioactivity. Optical imaging of amyloid fibrils using fluorescent tracers has attracted significant attention in recent years because of its simplicity, cost effectiveness, faster data accumulation, simple data analysis, and high sensitivity. Several small organic and inorganic molecules have been developed for the optical imaging of the amyloid fibrils. For example, Uchida et al. used Hoechst 33342 for detecting amyloid fibrils in APP transgenic mice.[17] Sensors based on fluorescein,[18] BODIPYs,[19,20] curcumin,[21] thiophene,[22] binuclear metal complexes,[23] etc were used for amyloid fibril detection. Interestingly, gold metal nanoparticles[24] and silicon nanoarrays[25] were also developed for the same purpose.

Intensive efforts notwithstanding, thioflavin-T (ThT) still remains the exclusive fluorescent probe for amyloid fibrils.[26–28] ThT, a nonemissive species in water, shows a very large increase ($>10^3$ times) in its emission yield on binding with the amyloid fibrils.[26] The increased emission yield of ThT has been attributed to the restriction in the nonradiative torsional motion around its central C–C single bond in the amyloid fibrils.[29,30] ThT lacks protein-specificity as it binds to amyloid fibrils made up from all classes of proteins. Nonetheless, it has

[a] A. K. Mora, S. Murudkar, A. Alamelu, Dr. P. K. Singh, Dr. S. Nath
Radiation & Photochemistry Division, Bhabha Atomic Research Centre
Trombay, Mumbai 400 085 (India)
E-mail: snath@barc.gov.in
sukhendunath@yahoo.co.in

[b] Dr. S. Chattopadhyay
Bio-organic Division, Bhabha Atomic Research Centre
Trombay, Mumbai 400 085 (India)

[c] A. Alamelu
Present address: Cardomom Planters Association College
Bodinayakanur, Tamil Nadu (India)

Supporting information for this article is available on the WWW under http://dx.doi.org/10.1002/chem.201602981.

been used for several decades for its high association constant with the amyloid fibrils, and large sensitivity due to the enormous increase in its emission intensity on association with amyloid fibrils. The actual mechanism for such a strong association of ThT with amyloid fibrils is still not clearly understood. It is believed that the molecular shape of ThT matches with that of some of the grooves in the fibrillar channel and on its surface.[31] Such shape complementarity between ThT and the amyloid structure along with the hydrophobic stabilization is believed to be mainly responsible for the strong association between ThT and amyloid fibrils. However, ThT cannot be employed for in vivo imaging due to its positive charge, which makes it highly hydrophilic and prevents it from crossing the blood–brain barrier (BBB).[32] Further, the spectral position of ThT remains largely unchanged on association with amyloid fibrils, which makes it inappropriate for the imaging studies due to the large background signal.[30,33] Moreover, ThT has been recently shown to promote amyloid β aggregation.[34] Such limitations of ThT have encouraged the development of neutral fluorescent sensors for amyloid fibrils.[32,35,36] However, sensors with molecular shapes similar to ThT are anticipated to provide extra selectivity due to structural complementarity between the fibrils and the probes. Thus, several neutral ThT derivatives were synthesized that showed a high affinity towards amyloid fibrils.[32,35–37] Derivatives based on radio-labeled bezothiazoleaniline (BTA) moieties are the most prolific and promising amyloid sensors, and have been used for the PET imaging of amyloid fibrils.[32,37] However, due to lack of suitable photophysical properties, such derivatives could not be used for the detection of amyloid fibrils using sensitive fluorescence techniques. Klunk et al. reported that BTA derivatives did not show any change in their emission spectrum on association with amyloid fibrils.[32] Instead, emission intensity of one of the BTA derivatives, which is extensively used for PET amyloid imaging, was reduced in the amyloid fibrillar solution.[37] Hence, a neutral ThT derivative, which can show a significant increase in its emission intensity along with the shift in the spectral position on association with amyloid fibrils, needs to be developed for efficient detection of these neurotoxic protein agglomerates.

In the present study, we synthesized a neutral analogue of ThT, 2-[2′-Me,4′-(dimethylamino)phenyl]benzothiazole (2Me-DABT, see Scheme 1 for the chemical structure), which showed a large change in its photophysical properties on association with amyloid fibrils made from insulin. The interaction of 2Me-DABT with insulin amyloid fibrils was studied using both steady-state and time-resolved fluorescence techniques. It is shown that unlike ThT, 2Me-DABT showed a significant blueshift in the emission spectrum along with a largely increased emission intensity due to its association with the amyloid fibrils, which suggests its potential application as a ratiometric amyloid fibril sensor. Fluorescence resonance energy transfer (FRET) and molecular docking studies were also performed to identify its binding sites in amyloid fibrils.

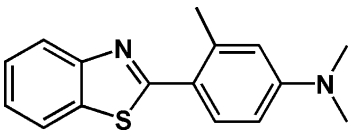

Scheme 1. Molecular structure of (2-[2′-Me,4′-(dimethylamino)phenyl]benzothiazole) (2Me-DABT).

Results and Discussion

2Me-DABT in aqueous solution showed a relatively narrow absorption band with a maxima at approximately 300 nm, which was largely unchanged in the presence of insulin amyloid fibrils (see Figure S1 in the Supporting Information). The emission spectra of 2Me-DABT, recorded in aqueous solution and in the presence of different concentrations of insulin fibrils, are shown in Figure 1. 2Me-DABT showed a broad emission band with maxima at 500 nm in aqueous solution. It is evident from Figure 1 that the addition of insulin fibrils to the aqueous solution of 2Me-DABT led to a substantially increased (≈65 times) emission intensity along with a significant hypsochromic shift in the emission spectrum. The inset of Figure 1 shows the peak intensity normalized emission spectra of 2Me-DABT in the presence of different concentrations of amyloid fibrils. The emission maxima of 2Me-DABT changed from 500 nm in aqueous solution to 445 nm in amyloid fibrils. The observed large fluorescence enhancement along with large blueshift in the emission spectra clearly indicated that 2Me-DABT interacts strongly with amyloid fibrils. It is noteworthy that despite having a strong interaction with amyloid fibrils, unlike ThT, the fibrillation kinetics of insulin remained unaffected by the presence of 2Me-DABT (see Figure S2 in the Supporting Information). Thus, the present result suggested that 2Me-DABT may be an efficient fluorescence sensor for the amyloid fibrils. In particular, the large shift in the emission spectra is advantageous for fluorescence imaging applications due to the relatively low background signal. This may also improve the detection limit significantly.

Such a large shift in the emission spectra of 2Me-DABT upon binding with amyloid fibrils can make it a ratiometric sensor for the amyloid fibrils. It is worth mentioning that the emission spectral position of ThT remains unchanged on association

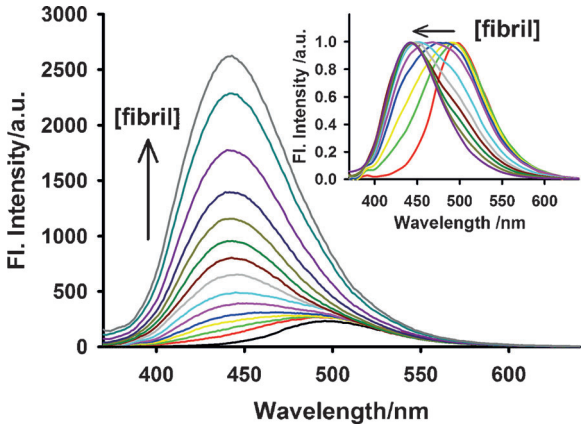

Figure 1. Emission spectra (λ_{ex} = 340 nm) of 2Me-DABT in the presence of different concentrations of insulin amyloid fibrils (0–30 μM). Inset: peak intensity normalized emission spectra of 2Me-DABT in amyloid fibrils.

with amyloid fibrils[26,30] and hence can act only as a single intensity based sensor. Such a single-intensity-based estimation is prone to error caused by the fluctuation in probe concentration and its environment, drift in the opto-electronic setup, etc. during the measurement.[38] However, the ratio of emission intensities of the probe at two different wavelengths is immune to such changes during the measurements.[38] Ratiometric measurements are particularly very important in microscopic studies of cells, for which the concentration and environment of probes as well as the optical path fluctuates continuously during the course of the measurement. It is also important to mention that the light used for the excitation of 2Me-DABT can generate autofluorescence from cells[39] and can interfere with the measurements. However, due to the very high emission quantum yield of 2Me-DABT in amyloid fibrils (68%), it is quite expected that the emission intensity generated from 2Me-DABT in amyloid fibrils will be significantly higher than that of cell autofluorescence. Hence, in microscopic studies using 2Me-DABT as a fibrillar probe, the interference from the cell autofluorescence is expected to be negligible.

To quantify the interaction between 2Me-DABT and insulin amyloid fibrils, binding constants were estimated by using the following modified Benesi–Hildebrand equation for 1:1 complexation:[40,41]

$$\frac{1}{\Delta I_f} = \frac{1}{K_b(I_C - I_O)[F]_o} + \frac{1}{(I_C - I_O)} \quad (1)$$

in which I_o and I_C are the emission intensities of 2Me-DABT in water and when completely bound with amyloid fibrils, respectively. ΔI_f is the change in the emission intensity due to the addition of fibrils. $[F]_0$ is the total concentration of fibrils in the solution and K_b is the binding constant. The double reciprocal plot for the variation in the emission intensity of 2Me-DABT with the concentration of amyloid fibrils is shown in Figure 2. The nonlinearity observed in Figure 2 clearly indicated two modes of binding for 2Me-DABT with amyloid fibrils. The experimental data were fitted with Equation (1) at two different concentration regions as shown in Figure 2. The binding constants thus estimated from the fitting, were found to be 1.0×10^6 and $4.1\times10^4\ M^{-1}$. Earlier, ThT was reported to follow two modes of binding, one in the fibrillar channel and the other in the grooves of the fibrillar surface.[42–44] Due to structural complementarity between ThT and the fibrillar channel, the binding in the inner channel of the fibrils is very strong compared to that on the surface. Considering the similar chemical structure of ThT and 2Me-DABT, in analogy, we also propose that the stronger binding mode corresponds to the 2Me-DABT bound to the inner channel of the fibril and the weaker mode is due to the binding of 2Me-DABT onto the fibrillar surface. This proposition was also supported by our molecular docking studies (vide infra).

Time-resolved emission measurements were performed to understand the effect of amyloid fibrils on the excited-state dynamics of 2Me-DABT. Figure 3A shows measured emission transient decays of 2Me-DABT in the presence of different concentrations of amyloid fibrils. The emission transient of 2Me-DABT in aqueous solution showed nonexponential decay kinetics. All transient decay traces were fitted with a biexponential decay function. The average lifetime (τ_{av}) of 2Me-DABT in aqueous solution was estimated to be 2.9 ns. It is to be noted from Figure 3A that the emission transient decay became gradually slower on addition of amyloid fibrils. The variation in the average lifetimes of 2Me-DABT with amyloid fibril concentrations are presented in Figure 3B. It is evident from Figure 3B that the average excited-state lifetime of 2Me-DABT was increased from 2.9 ns in water to 4.3 ns in the presence of 25 μM amyloid fibrils. Such changes in the excited-state lifetime certainly indicated a strong interaction of 2Me-DABT with amyloid fibrils. As time-resolved measurements are inherently ratiometric in nature, the changes in the lifetime of 2Me-DABT can also be used for the estimation of amyloid fibrils. However, it is to be noted that the steady-state emission intensity of 2Me-DABT was changed by approximately 65 times due to its association with amyloid fibrils, whereas its lifetime changed only by 1.5 times. Hence, for the present system, the emission-intensity-based detection of amyloid fibrils will be more sensitive than the lifetime-based method.

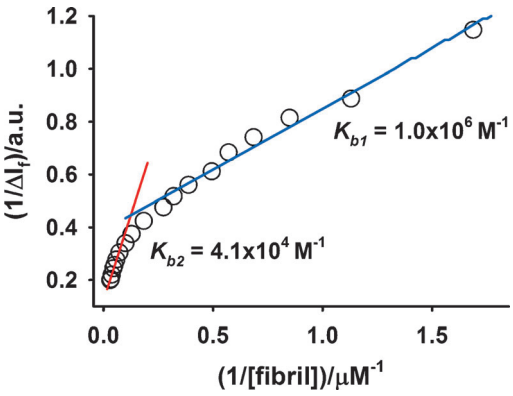

Figure 2. Double reciprocal plot for the variation in emission intensity of 2Me-DABT with the concentration of insulin amyloid fibrils. The two straight lines are the fit for the experimental data by using Equation (1).

To comprehend the reason for the observed changes in the emission characteristics of 2Me-DABT due to its interaction with amyloid fibrils, emission properties of 2Me-DABT in different solvents were investigated in detail. The emission spectra of 2Me-DABT recorded in acetonitrile/water solvent mixtures are shown in Figure 4A. A substantial decrease in the emission intensity of 2Me-DABT was noticed with the increase in the solvent polarity. The peak intensity normalized emission spectra of 2Me-DABT in solvent mixtures are shown in the inset of Figure 4A. The emission spectrum of 2Me-DABT showed a large bathochromic shift on increasing the solvent polarity. Thus, the emission maxima of 2Me-DABT in acetonitrile (dielectric constant, $\varepsilon = 37.5$) is 463 nm and changed to 495 nm in a 95% water/acetonitrile mixture ($\varepsilon = 76$).[45,46] Due to the extremely low solubility of 2Me-DABT in water, its photophysical properties in neat water could not be studied. On changing the solvent from neat acetonitrile to a 95% water/acetonitrile mixture, 2Me-DABT showed a Stokes's shift (1391 cm^{-1}), which was quite large when compared to commonly used solvatochromic

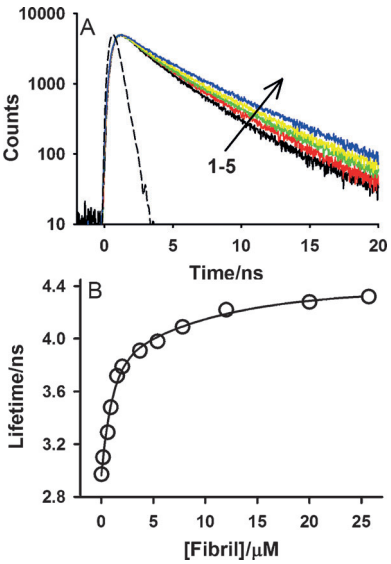

Figure 3. A) Emission transient decays for 2Me-DABT in the presence of different concentrations of insulin amyloid fibrils: 1) 0, 2) 0.6, 3) 4.5, 4) 12, and 5) 20 μM. The dashed curve represents the instrument response function (IRF) of the TCSPC instrument. B) Variation in the average lifetime of 2Me-DABT with insulin amyloid fibril concentration.

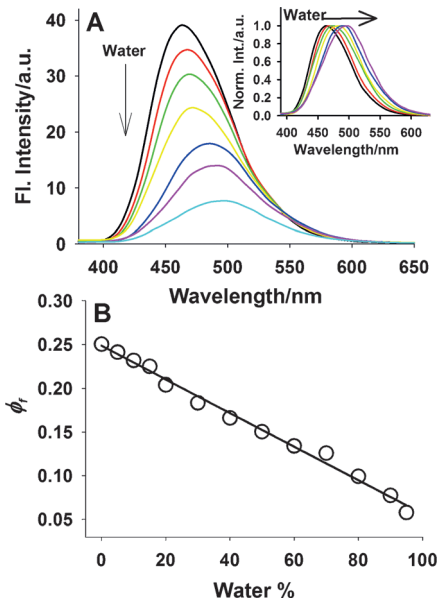

Figure 4. A) Emission spectra of 2Me-DABT in acetonitrile in the presence of different amounts of water. Inset: the peak normalized emission spectra of 2Me-DABT in acetonitrile/water solvent mixtures. B) Variation in the emission quantum yield of 2Me-DABT with the percentage of water in acetonitrile/water mixtures.

dyes, like coumarin 153 (1031 cm^{-1}). Thus, present results indicated that 2Me-DABT is a strong solvatochromic dye and may be a potential candidate to probe the micropolarity of different complex chemical and biological environments. Figure 4B shows the variation in the emission quantum yield (ϕ_f) of 2Me-DABT with solvent polarity. Thus, the emission yield of 2Me-DABT was decreased substantially with the increase in the water content in mixed solvents. This result clearly indicated that nonradiative deactivation of 2Me-DABT became more prominent in the high-polarity solvent media.

From above results it can be inferred that a decrease in the polarity around 2Me-DABT led to a blueshift in its emission spectrum and a simultaneous increase in its emission yield. Due to their extremely complex structure, amyloid fibrils can have different hydrophobic pockets to accommodate small molecules. For example, Nile red on its association with amyloid fibrils experienced much lower polarity when compared to the bulk water, which is reflected by the blueshift in its emission spectra.[47] Thus, it can be inferred that the micropolarity at the site of solubilization of 2Me-DABT in amyloid fibrils is much less as compared to the bulk water. Such a low polarity around 2Me-DABT in the fibrillar media resulted in a significant blueshift in its emission spectra with a concomitant large increase in its emission yield.

As 2Me-DABT has a very similar molecular structure to ThT, it was important to know whether these two amyloid probes have similar or independent binding sites in the insulin amyloid fibrils. For this, we investigated the emission characteristics of 2Me-DABT in a fibrillar solution in the presence of different concentrations of ThT. There was a substantial decrease in the emission intensity of 2Me-DABT at 445 nm, on addition of ThT to the fibrillar solution (Figure 5). Such a decrease in the emission intensity of 2Me-DABT is also accompanied by a large increase in the emission at 490 nm due to ThT bound to amyloid fibrils.[30] The emission spectrum for only ThT in fibrillar media is also shown in Figure 5 for comparison. The emission intensity of only ThT in amyloid fibrils was quite low when excited at 340 nm. However, the emission of ThT at 490 nm is significantly enhanced in the presence of 2Me-DABT in amyloid fibrils. The variation in the emission intensities at 445 and 490 nm as a function of ThT concentration are also shown in the inset of Figure 5. The large increase in the emission intensity at 490 nm at the cost of that at 445 nm clearly indicated an efficient energy transfer from the photoexcited 2Me-DABT to ThT in the fibrillar media. The energy-transfer process is further supported by the fact that there was a substantial overlap between the emission spectrum of 2Me-DABT and the absorption spectrum of ThT in the fibrillar media (see Figure S3 in the Supporting Information).

Observed energy transfer between the photoexcited 2Me-DABT to ThT clearly indicated that ThT could not replace the 2Me-DABT from amyloid fibrils. Rather, the added ThT occupied some other suitable available sites in amyloid fibrils without replacing the preoccupied 2Me-DABT. In fact, it is quite expected that amyloid fibrils made from large proteins, like insulin, will have large numbers of binding sites such that even if some of the sites are occupied by one probe, the other probe can find another energetically suitable site without replacing the first probe. Additionally, our studies further confirmed that the binding sites for ThT and 2Me-DABT are proximal enough for an efficient FRET between them, which is further supported by our molecular docking studies discussed in the later part.

The FRET between photoexcited 2Me-DABT and ThT in the fibrillar solution has also been studied by time-resolved fluorescence measurements. The emission transient decay of 2Me-

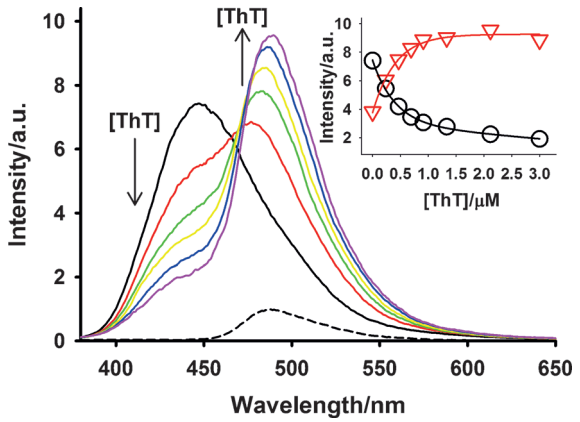

Figure 5. Emission spectra (λ_{ex} = 340 nm) of 2Me-DABT in insulin amyloid fibrillar solution in the presence of different concentrations of ThT (0–3 μM). The dashed curve shows the emission spectrum (λ_{ex} = 340 nm) of 3 μM ThT in the fibrillar solution. Inset: variation in the emission intensity at (circles) 445 and (triangles) 490 nm with ThT concentration in the fibrillar solution.

DABT in fibrillar solution became faster with the increase in ThT concentration (cf. Figure 6). It is important to mention that no ThT emission at 445 nm from fibrillar solution was observed on photoexcitation with 340 nm light. Hence, emission decays recorded at 445 nm were solely from the photoexcited 2Me-DABT bound to amyloid fibrils. It is evident from Figure 6 that the addition of ThT to the fibrillar solution led to quenching of the excited state of 2Me-DABT. Thus, the average lifetime of 2Me-DABT in insulin amyloid fibrils was shortened from 4.3 to 1.7 ns in the presence of 3 μM ThT. Overall, the time-resolved emission studies further supported the energy transfer from photoexcited 2Me-DABT to ThT molecules in the fibrillar solution. The efficiency (E) for the FRET between photoexcited 2Me-DABT and ThT in the fibrillar solution was calculated using the following equation and found to be 60.5 %:[48]

$$E = 1 - \frac{\langle \tau_{DA} \rangle}{\langle \tau_{D} \rangle} \qquad (2)$$

in which $\langle \tau_{DA} \rangle$ and $\langle \tau_{D} \rangle$ are the amplitude-weighted lifetimes [cf. Eq. (5)] of fibril-bound 2Me-DABT in the presence and absence of ThT, respectively. Using this E value, the average separation between 2Me-DABT and ThT was calculated to be 41.2 Å (see the Supporting Information for detailed calculations). Such a large separation between ThT and 2Me-DABT further suggested that these two amyloid probes did not share the same localization site in the amyloid fibrils, as indicated by the results of the steady-state emission studies.

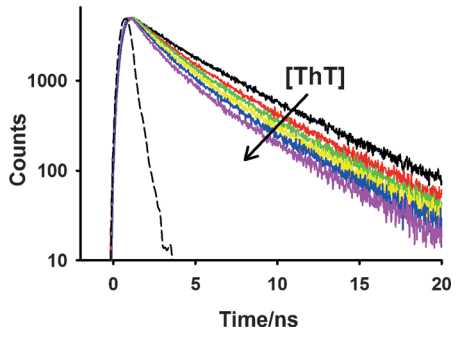

Figure 6. Emission transient decays for insulin amyloid fibril-bound 2Me-DABT in the presence of different ThT concentrations (0–3 μM). The dashed curve represents the IRF.

The knowledge of binding sites of the probes is very important to understand their sensory activity and for future sensor development. Hence, we performed the blind molecular docking studies to find out the location of 2Me-DABT in amyloid fibrils. Due to lack of detail structural information on insulin amyloid fibrils, in the present docking studies, we used the fibrillar structure for 42 residue amyloid-β protein ($A\beta_{1-42}$) determined by solid-state NMR (PDB ID: 2MXU).[49] The use of the $A\beta_{1-42}$ fibril rather than fibril of the most abundant 40 residue amyloid-β protein ($A\beta_{1-40}$) in the present work was motivated from the fact that the protofibril of the $A\beta_{-42}$ protein is much more toxic and showed more propensity towards aggregation compared to the $A\beta_{1-40}$ protein.[50,51] Docking of 2Me-DABT in $A\beta_{1-42}$ fibril was performed with several initial positions of ligand with respect to the host fibril. The initial docking consisted of 1000 runs, and all the results were clustered with a RMSD value of 2 Å. After clustering, two primary binding sites for 2Me-DABT in $A\beta_{1-42}$ fibrils were identified. These two most-probable and lowest-energy binding conformations involved localization of 2Me-DABT in the inner channel of fibrils (Figure 7 A). The binding energies for mode-1 (with a population 750 out of 1000) and mode-2 (with a population 180 out of 1000) were estimated to be 6.87 and 6.39 kcal mol^{-1}, respectively. Different interactions operating between 2Me-DABT and the amino acids of amyloid fibrils for most populated mode of binding (mode-1) are shown in Figure 7 B. It was found that the binding of 2Me-DABT in the amyloid fibrils was mainly supported by the π–π stacking interaction between the aromatic rings of 2Me-DABT and the nearby histidine moiety (His14). Further, the π–π interaction between the aromatic rings of 2Me-DABT with amide bonds of amyloid fibrils was also operative in the binding process. Besides, the hydrophobic interaction with the CH_2 groups of the peptide chain also favored the incorporation of 2Me-DABT in the inner-core region of the fibrils. In addition, binding at the external grooves of the fibrils was also observed in the present system (see Figure S4 in the Supporting Information). The population of such surface groove binding was extremely low (6 out of 1000) with a relatively low binding energy (5.45 kcal mol^{-1}). Importantly, unlike ThT, binding of 2Me-DABT at two ends of the fibrils could not be observed in our docking studies.[52] The results are in agreement with the simulation results reported by Wu et al., who showed that the probability of binding at two ends of the beta-sheet structure is much higher for ThT compared to its neutral analogues.[53]

To further identify the relative location of 2Me-DABT and ThT in amyloid fibrils, we performed molecular docking using the fibril with docked 2Me-DABT (mode-1) as the initial host structure. The most populated and the strongest mode of binding showed that the added ThT is also localized in the inner core of the fibril. The relative position of ThT with respect to 2Me-

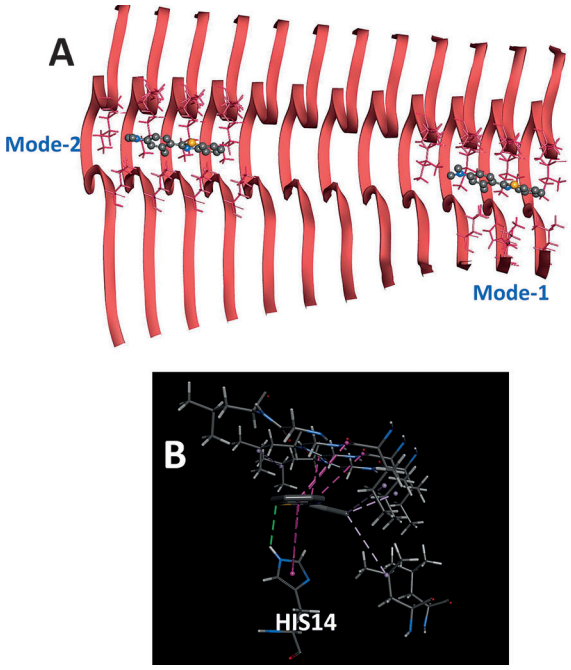

Figure 7. A) The two most probable binding sites for 2Me-DABT in amyloid fibrils obtained from the molecular docking studies. B) A close look of the binding pocket for mode-1. The dashed lines indicated different types of interaction involved between 2Me-DABT and fibril.

DABT in the amyloid fibrils is shown in Figure 8. Our docking studies showed that ThT was separated from 2Me-DABT by 40.2 Å. The distance between 2Me-DABT and ThT, obtained from the molecular docking studies is very close to the values obtained from the FRET studies. Our docking studies further supported the fact that the site of localization of 2Me-DABT and ThT are quite different as proposed in the previous section.

Conclusions

The newly synthesized neutral benzothiazole derivative, 2Me-DABT, binds strongly with the amyloid fibrils resulting in a large increase in its emission intensity along with a large spectral shift. Thus, unlike most extensively used amyloid sensors, such as ThT, a large shift in the emission wavelength of 2Me-DABT upon binding to amyloid fibrils makes it a potential ratiometric sensor and hence can provide high sensitivity in the detection of amyloid fibrils by fluorescence imaging techniques. Detailed spectroscopic studies indicated that the large changes in the emission properties of 2Me-DABT in amyloid fibrils was due to low polarity of the hydrophobic pockets in amyloid fibrils in which 2Me-DABT resided. FRET and molecular docking studies confirmed that the binding locations for ThT and 2Me-DABT are distinct and separated from each other by an average distance of approximately 40 Å. Further, as a neutral molecule, 2Me-DABT may be more efficient for in vivo imaging of amyloid fibrils. The knowledge on the binding sites and mode of interaction between probe and fibrils, obtained from the present study, will help in understanding the interaction of benzothiazole-based small molecules with amyloid fibrils.

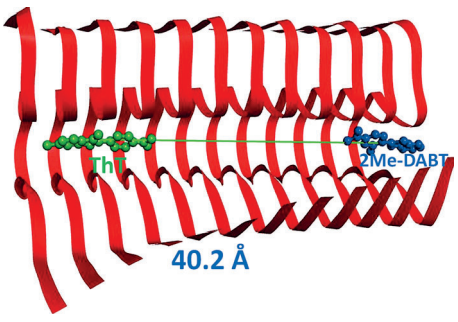

Figure 8. Binding pose of ThT in the amyloid fibril with incorporated 2Me-DABT. The solid line indicates the distance between 2Me-DABT and ThT.

Experimental Section

The ground-state absorption and the steady-state emission spectra were recorded using a Jasco spectrophotometer (model V-530) and Hitachi spectrofluorometer (model F4500), respectively. Fluorescence quantum yield (ϕ_f) values were estimated by a comparative method[48] using 4′,6-diamidino-2-phenylindole (DAPI) in dimethyl sulfoxide as the reference ($\phi_f \approx 0.58$).[54] In steady-state emission studies, 2Me-DABT was excited at 340 nm to avoid the emission from insulin protein. The time-resolved emission measurements were performed using a time-correlated single-photon counting (TCSPC)-based spectrometer from IBH, UK, as described earlier.[55] In time-resolved experiments, samples were excited with a 340 nm LED source. The instrument response function (IRF) of the TCSPC instrument was 1.3 ns. All decay traces were fitted by following multiexponential function.

$$I(t) = \sum_i a_i e^{-t/\tau_i} \quad (3)$$

in which, τ_i and a_i are the time constant and relative contribution of the *i*th decay component to the measured decay traces, respectively. Time (τ_{av}) and amplitude ($\langle\tau\rangle$)-weighted average lifetimes were calculated using the following equations.[48]

$$\tau_{av} = \frac{\sum_i a_i \tau_i^2}{\sum_i a_i \tau_i} \quad (4)$$

$$\langle\tau\rangle = \frac{\Sigma_i a_i \tau i}{\Sigma_i a_i} \quad (5)$$

Bovine insulin was obtained from Sigma. ThT was purchased as its chloride salt from Sigma and purified by recrystalization from a methanol/water mixture. Double-distilled water (conductivity < 0.1 mS cm^{-1}) was used for the sample preparation. All chemicals used for the synthesis were of analytical grade. Due to extremely low solubility of 2Me-DABT in neat water, its aqueous solution was prepared by using a concentrated stock solution in methanol such that the methanol content in the final solution was < 0.5% by volume. In all experiments, absorbance of 2Me-DABT solution was in the range 0.01–0.02 at 300 nm.

Insulin fibrils were prepared by following the procedure reported in the literature.[30,56] Insulin solution (2 mg mL^{-1}) in 20% acetic acid (pH 1.6) was heated at 70 °C for 24 h without stirring. The completion of the fibrillation process was monitored through the standard ThT fluorescence assay. Fibrils, thus prepared in the acidic

medium, were diluted 12-fold with Tris-HCl buffer and the pH was adjusted to 7.4 with aqueous NaOH solution.

Synthesis of 2Me-DABT

The preparation of 2Me-DABT is outlined in Scheme 2.

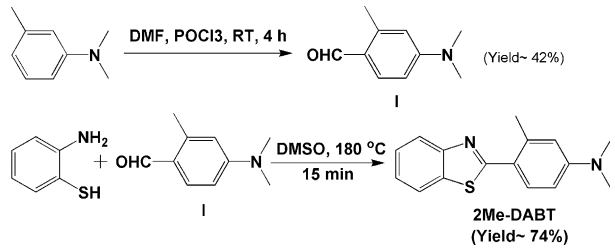

Scheme 2. Synthesis of 2Me-DABT.

4-(Dimethylamino)-2-methylbenzaldehyde (I)

Phosphorous oxychloride (0.78 mL, 8.1 mM) was added dropwise under an argon atmosphere to a cooled (−10 °C) and stirred solution of *N,N*-3-trimethylaniline (1.1 mL, 7.4 mM) and *N,N*-dimethylformamide (0.7 mL, 8.9 mM) in dichloromethane (40 mL). The reaction mixture was brought to room temperature, stirred for 4 h, treated with aqueous 2 M sodium hydroxide, and stirred for 4 h followed by the extraction with ethyl acetate. The organic extract was washed with water and brine, dried, concentrated in vacuo, and the residue purified by column chromatography (silica gel) to give the desired aldehyde (0.5 g, 41.6%). ^{1}H NMR (200 MHz, $CDCl_3$): $\delta =$ 2.36 (s, 3H), 2.9 (s, 6H), 6.80–6.84 (d, 2H, $J = 8.0$ Hz), 7.65 (d, 1H, $J = 8.0$ Hz), 10.14 ppm (s, 1H).

2Me-DABT

2-Aminothiophenol (0.49 g, 4.0 mM) was added to a stirred solution of **I** (3.1 mM) in dimethyl sulfoxide (25 mL) and the reaction mixture was heated at 180 °C for 15 min. After cooling to room temperature, the mixture was poured into water and extracted with ethyl acetate. The organic layer was washed with water and brine, and dried. Removal of the solvent in vacuo produced a yellow solid, which was purified by column chromatography (silica gel) to give pure 2Me-DABT (0.61 g, 74%). ^{1}H NMR (200 MHz, $CDCl_3$): $\delta = 2.39$ (s, 3H), 2.73 (s, 6H), 7.02–7.10 (m, 2H), 7.29–7.33 (m, 1H), 7.36–7.48 (m, 1H), 7.87 (d, 1H, $J = 8$ Hz), 8.03 (d, 1H, $J =$ 8 Hz), 8.24 ppm (d, 1H, $J = 8$ Hz).

Computational methods

AutoDock suite (version 4.2)[57] implemented in the AutoDock Tools (version 1.5.6)[58] was used for the molecular docking studies. The structure of $A\beta_{1-42}$ fibril was obtained from the PDB data bank (PDB ID: 2MXU). The structures of 2Me-DABT and ThT were energy-optimized by quantum chemical calculations using a Gaussian 03 package.[59] B3LYP functional[60,61] and 6-311++g(d,p) basis function were used to optimize the chemical structures by DFT. The energy-optimized structure of 2Me-DABT and ThT are shown in Figure S5 in the Supporting Information and used for blind docking studies. For docking studies, fibril was considered as a rigid host molecules and 2Me-DABT as a flexible ligand allowing all torsional motion in the molecule. Molecular docking was performed with five different initial locations of the ligand with respect to the fibril. A cubical box with dimensions of $100 \times 100 \times 100$ Å^3 with 0.6 Å grid spacing was created at the center of the fibril. The size of the grid box was made in such that the ligand can access all possible binding sites in fibrils. Each docking involved 200 independent runs with a maximum number of 5×10^6 energy evaluation and 27000 generations. The Lamarckian genetic algorithm (LGA)[62] method was applied to find the docked conformations of the ligand with the lowest energy. Results of all 1000 runs were clustered with root mean square deviation (RMSD) < 2 Å and ranked according to their binding energies. For docking with ThT, fibril with a docked 2Me-DABT was used as the host molecule. A similar procedure as used for the docking of 2Me-DABT with fibril was followed.

Acknowledgements

We are thankful to Prof. A. Datta, Indian Institute of Technology, Bombay, for his help in quantum chemical calculations. A.A. is thankful to the Indian Science Academies (IASC, INSA & NASI) for the summer research fellowship. S.M. thanks the Board of Research in Nuclear Sciences (BRNS) for a scholarship.

Keywords: amyloid fibrils · biosensors · fluorescent probes · thioflavin-T · time-resolved spectroscopy

[1] J. D. Sipe, *Annu. Rev. Biochem.* **1992**, *61*, 947–975.
[2] L. C. Serpell, *Biochim. Biophys. Acta Mol. Basis Dis.* **2000**, *1502*, 16–30.
[3] F. Chiti, C. M. Dobson, *Annu. Rev. Biochem.* **2006**, *75*, 333–366.
[4] D. R. Booth, M. Sunde, V. Bellotti, C. V. Robinson, W. L. Hutchinson, P. E. Fraser, P. N. Hawkins, C. M. Dobson, S. E. Radford, C. C. Blake, M. B. Pepys, *Nature* **1997**, *385*, 787–793.
[5] S. J. Hubbard, *Biochim. Biophys. Acta Protein Struct. Mol. Enzymol.* **1998**, *1382*, 191–206.
[6] J. D. Sipe, A. S. Cohen, *J. Struct. Biol.* **2000**, *130*, 88–98.
[7] A. Lomakin, D. S. Chung, G. B. Benedek, D. A. Kirschner, D. B. Teplow, *Proc. Natl. Acad. Sci. USA* **1996**, *93*, 1125–1129.
[8] C. L. Oliveira, M. A. Behrens, J. S. Pedersen, K. Erlacher, D. Otzen, *J. Mol. Biol.* **2009**, *387*, 147–161.
[9] G. Zandomeneghi, M. R. H. Krebs, M. G. McCammon, M. Fändrich, *Protein Sci.* **2009**, *13*, 3314–3321.
[10] S. Guo, B. B. Akhremitchev, *Biomacromolecules* **2006**, *7*, 1630–1636.
[11] D. Yanagisawa, H. Taguchi, N. F. Ibrahim, S. Morikawa, A. Shiino, T. Inubushi, K. Hirao, N. Shirai, T. Sogabe, I. Tooyama, *J. Alzheimers Dis.* **2014**, *39*, 617–631.
[12] M. Higuchi, N. Iwata, Y. Matsuba, K. Sato, K. Sasamoto, T. C. Saido, *Nat. Neurosci.* **2005**, *8*, 527–533.
[13] W. E. Klunk, H. Engler, A. Nordberg, Y. Wang, G. Blomqvist, D. P. Holt, M. Bergström, I. Savitcheva, G.-F. Huang, S. Estrada, B. Ausén, M. L. Debnath, J. Barletta, J. C. Price, J. Sandell, B. J. Lopresti, A. Wall, P. Koivisto, G. Antoni, C. A. Mathis, B. Långström, *Ann. Neurol.* **2004**, *55*, 306–319.
[14] A. Nordberg, *Lancet Neurol.* **2004**, *3*, 519–527.
[15] W. Zhen, H. Han, M. Anguiano, C. A. Lemere, C.-G. Cho, P. T. Lansbury, Jr., *J. Med. Chem.* **1999**, *42*, 2805–2815.
[16] Y. Wang, W. E. Klunk, M. L. Debnath, G.-F. Huang, D. P. Holt, L. Shao, C. A. Mathis, *J. Mol. Neurosci.* **2004**, *24*, 55–62.
[17] Y. Uchida, H. Takahashi, *Neurosci. Lett.* **2008**, *448*, 279–281.
[18] D. Allsop, L. Swanson, S. Moore, Y. Davies, A. York, O. M. A. El-Agnaf, I. Soutar, *Biochem. Biophys. Res. Commun.* **2001**, *285*, 58–63.
[19] M. Ono, H. Watanabe, H. Kimura, H. Saji, *ACS Chem. Neurosci.* **2012**, *3*, 319–324.
[20] A. Ojida, T. Sakamoto, M.-A. Inoue, S.-H. Fujishima, G. Lippens, I. Hamachi, *J. Am. Chem. Soc.* **2009**, *131*, 6543–6548.
[21] C. Ran, X. Xu, S. B. Raymond, B. J. Ferrara, K. Neal, B. J. Bacskai, Z. Medarova, A. Moore, *J. Am. Chem. Soc.* **2009**, *131*, 15257–15261.

[22] R. Chandra, M.-P. Kung, H. F. Kung, *Bioorg. Med. Chem. Lett.* **2006**, *16*, 1350 – 1352.
[23] V. Sathish, E. Babu, A. Ramdass, Z.-Z. Lu, M. Velayudham, P. Thanasekaran, K.-L. Lu, S. Rajagopal, *Talanta* **2014**, *130*, 274 – 279.
[24] C. Wang, D. Liu, Z. Wang, *Chem. Commun.* **2012**, *48*, 8392 – 8394.
[25] P. Gagni, L. Sola, M. Cretich, M. Chiari, *Biosens. Bioelectron.* **2013**, *47*, 490 – 495.
[26] H. LeVine III, *Protein Sci.* **2008**, *2*, 404 – 410.
[27] M. Groenning, *J. Chem. Biol.* **2010**, *3*, 1 – 18.
[28] M. Biancalana, S. Koide, *Biochim. Biophys. Acta Proteins Proteomics* **2010**, *1804*, 1405 – 1412.
[29] A. Srivastava, P. K. Singh, M. Kumbhakar, T. Mukherjee, S. Chattopadyay, H. Pal, S. Nath, *Chem. Eur. J.* **2010**, *16*, 9257 – 9263.
[30] P. K. Singh, M. Kumbhakar, H. Pal, S. Nath, *J. Phys. Chem. B* **2010**, *114*, 2541 – 2546.
[31] C. Rodríguez-Rodríguez, A. Rimola, L. Rodríguez-Santiago, P. Ugliengo, A. Álvarez-Larena, H. Gutiérrez-De-Terán, M. Sodupe, P. González-Duarte, *Chem. Commun.* **2010**, *46*, 1156 – 1158.
[32] W. E. Klunk, Y. Wang, G. F. Huang, M. L. Debnath, D. P. Holt, C. A. Mathis, *Life Sci.* **2001**, *69*, 1471 – 1484.
[33] A. A. Maskevich, V. I. Stsiapura, V. A. Kuzmitsky, I. M. Kuznetsova, O. I. Povarova, V. N. Uversky, K. K. Turoverov, *J. Proteome Res.* **2007**, *6*, 1392 – 1401.
[34] M. D'Amico, M. G. Di Carlo, M. Groenning, V. Militello, V. Vetri, M. Leone, *J. Phys. Chem. Lett.* **2012**, *3*, 1596 – 1601.
[35] R. L. Yona, S. Mazeres, P. Faller, E. Gras, *ChemMedChem* **2008**, *3*, 63 – 66.
[36] C. A. Mathis, B. J. Bacskai, S. T. Kajdasz, M. E. McLellan, M. P. Frosch, B. T. Hyman, D. P. Holt, Y. Wang, G.-F. Huang, M. L. Debnath, W. E. Klunk, *Bioorg. Med. Chem. Lett.* **2002**, *12*, 295 – 298.
[37] A. Lockhart, L. Ye, D. B. Judd, A. T. Merrittu, P. N. Lowe, J. L. Morgenstern, G. Hong, A. D. Gee, J. Brown, *J. Biol. Chem.* **2005**, *280*, 7677 – 7684.
[38] G. Grynkiewicz, M. Poenie, R. Y. Tsien, *J. Biol. Chem.* **1985**, *260*, 3440 – 3450.
[39] F. Crespi, A. C. Croce, S. Fiorani, B. Masala, C. Heidbreder, G. Bottiroli, *Lasers Surg. Med.* **2004**, *34*, 39 – 47.
[40] M. L. Benesi, J. H. Hildebrand, *J. Am. Chem. Soc.* **1949**, *71*, 2703 – 2707.
[41] S. Murudkar, A. K. Mora, S. Jakka, P. K. Singh, S. Nath, *J. Photochem. Photobiol. A* **2014**, *295*, 17 – 25.
[42] M. Groenning, M. Norrman, J. M. Flink, M. van de Weert, J. T. Bukrinsky, G. Schluckebier, S. Frokjaer, *J. Struct. Biol.* **2007**, *159*, 483 – 497.
[43] R. Sabaté, I. Lascu, S. J. Saupe, *J. Struct. Biol.* **2008**, *162*, 387 – 396.
[44] P. K. Singh, A. K. Mora, S. Nath, *Chem. Commun.* **2015**, *51*, 14042 – 14045.
[45] Dielectric constants (ε_{ms}) of the mixed solvents were calculated by using the equation $\varepsilon_{ms} = v_1\varepsilon_1 + v_2\varepsilon_2$, in which v_i and ε_i are the volume fraction and the dielectric constant of the constituent solvents; see reference [46].
[46] A. Barik, S. Nath, H. Pal, *J. Chem. Phys.* **2003**, *119*, 10202 – 10208.
[47] R. Mishra, D. Sjölander, P. Hammarström, *Mol. BioSyst.* **2011**, *7*, 1232 – 1240.
[48] J. R. Lackowicz, *Principles of fluorescence spectroscopy*, 3rd ed., Springer, New York, **2006**.
[49] Y. Xiao, B. Ma, D. McElheny, S. Parthasarathy, F. Long, M. Hoshi, R. Nussinov, Y. Ishii, *Nat. Struct. Mol. Biol.* **2015**, *22*, 499 – 505.
[50] L. M. Luheshi, G. G. Tartaglia, A.-C. Brorsson, A. P. Pawar, I. E. Watson, F. Chiti, M. Vendruscolo, D. A. Lomas, C. M. Dobson, D. C. Crowther, *PLoS Biol.* **2007**, *5*, e290.
[51] J. Davis, W. E. Van Nostrand, *Proc. Natl. Acad. Sci. USA* **1996**, *93*, 2996 – 3000.
[52] C. Wu, M. T. Bowers, J.-E. Shea, *Biophys. J.* **2011**, *100*, 1316 – 1324.
[53] C. Wu, Z. Wang, H. Lei, Y. Duan, M. T. Bowers, J.-E. Shea, *J. Mol. Biol.* **2008**, *384*, 718 – 729.
[54] T. Hard, P. Fan, D. R. Kearns, *Photochem. Photobiol.* **1990**, *51*, 77 – 86.
[55] A. K. Mora, P. K. Singh, S. Nath, *J. Phys. Chem. B* **2016**, *120*, 4143 – 4151.
[56] K. J. Robbins, G. Liu, V. Selmani, N. D. Lazo, *Langmuir* **2012**, *28*, 16490 – 16495.
[57] G. M. Morris, R. Huey, W. Lindstrom, M. F. Sanner, R. K. Belew, D. S. Goodsell, A. J. Olson, *J. Comput. Chem.* **2009**, *30*, 2785 – 2791.
[58] M. F. Sanner, *J. Mol. Graph. Model.* **1999**, *17*, 57 – 61.
[59] Gaussian 03, Revision C.01, M. J. Frisch, G. W. Trucks, H. B. Schlegel, G. E. Scuseria, M. A. Robb, J. R. Cheeseman, J. A. Montgomery, Jr., T. Vreven, K. N. Kudin, J. C. Burant, J. M. Millam, S. S. Iyengar, J. Tomasi, V. Barone, B. Mennucci, M. Cossi, G. Scalmani, N. Rega, G. A. Petersson, H. Nakatsuji, M. Hada, M. Ehara, K. Toyota, R. Fukuda, J. Hasegawa, M. Ishida, T. Nakajima, Y. Honda, O. Kitao, H. Nakai, M. Klene, X. Li, J. E. Knox, H. P. Hratchian, J. B. Cross, C. Adamo, J. Jaramillo, R. Gomperts, R. E. Stratmann, O. Yazyev, A. J. Austin, R. Cammi, C. Pomelli, J. W. Ochterski, P. Y. Ayala, K. Morokuma, G. A. Voth, P. Salvador, J. J. Dannenberg, V. G. Zakrzewski, S. Dapprich, A. D. Daniels, M. C. Strain, O. Farkas, D. K. Malick, A. D. Rabuck, K. Raghavachari, J. B. Foresman, J. V. Ortiz, Q. Cui, A. G. Baboul, S. Clifford, J. Cioslowski, B. B. Stefanov, G. Liu, A. Liashenko, P. Piskorz, I. Komaromi, R. L. Martin, D. J. Fox, T. Keith, M. A. Al-Laham, C. Y. Peng, A. Nanayakkara, M. Challacombe, P. M. W. Gill, B. Johnson, W. Chen, M. W. Wong, C. Gonzalez, J. A. Pople, Gaussian, Inc., Wallingford, CT, **2004**.
[60] A. D. Becke, *J. Chem. Phys.* **1993**, *98*, 5648 – 5652.
[61] C. Lee, W. Yang, R. G. Parr, *Phys. Rev. B* **1988**, *37*, 785 – 789.
[62] G. M. Morris, D. S. Goodsell, R. S. Halliday, R. Huey, W. E. Hart, R. K. Belew, A. J. Olson, *J. Comput. Chem.* **1998**, *19*, 1639 – 1662.

Received: June 22, 2016
Published online on ■■ ■■, 0000

FULL PAPER

Bound and determined: Neutral thioflavin-T derivative, 2Me-DABT, showed a large increase in its emission intensity as well as a significant blue shift in the emission spectrum due to its association with amyloid fibrils (see figure). Molecular docking studies confirmed the binding of 2Me-DABT in the inner core of the amyloid fibrils.

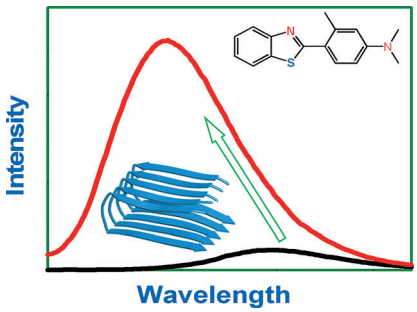

Fluorescent Amyloid Probe

*A. K. Mora, S. Murudkar, A. Alamelu, P. K. Singh, S. Chattopadhyay, S. Nath**

■■ – ■■

Benzothiazole-Based Neutral Ratiometric Fluorescence Sensor for Amyloid Fibrils